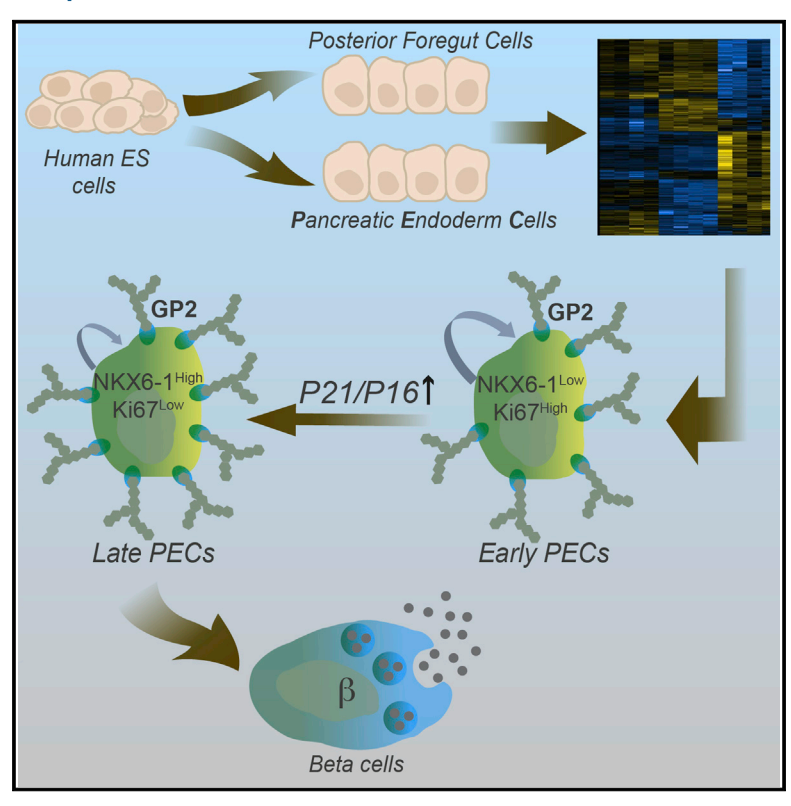
# **Cell Reports**

# **Efficient Generation of Glucose-Responsive Beta** Cells from Isolated GP2<sup>+</sup> Human Pancreatic **Progenitors**

# **Graphical Abstract**



# **Highlights**

- Genome-wide expression analysis reveals 115 genes specifically enriched in PECs
- Pure populations of PECs can be isolated using the cell surface marker GP2
- GP2<sup>+</sup> PECs differentiate with high efficiency into glucoseresponsive INS+ cells
- Reducing p21 or p16 expression enhances the proliferative capacity of PECs

# **Authors**

Jacqueline Ameri, Rehannah Borup, Christy Prawiro, Cyrille Ramond, Karen A. Schachter, Raphael Scharfmann, Henrik Semb

# Correspondence

semb@sund.ku.dk

#### In Brief

Ameri et al. identify GP2 as a specific marker of human pancreatic endoderm cells (PECs) and demonstrate that isolated GP2+ PECs generate cultures enriched in glucose-responsive insulinproducing cells. By eliminating undifferentiated hESCs, this work suggests a safer route toward manufacture of endocrine cells for future diabetes cell therapy.

# **Accession Numbers**

E-MTAB-5088









# Efficient Generation of Glucose-Responsive Beta Cells from Isolated GP2<sup>+</sup> Human Pancreatic Progenitors

Jacqueline Ameri, <sup>1,2</sup> Rehannah Borup, <sup>3</sup> Christy Prawiro, <sup>1</sup> Cyrille Ramond, <sup>4</sup> Karen A. Schachter, <sup>1</sup> Raphael Scharfmann, <sup>4</sup> and Henrik Semb<sup>1,2,5,\*</sup>

<sup>1</sup>The Danish Stem Cell Center (DanStem), Faculty of Health Sciences, University of Copenhagen, 2200 Copenhagen N, Denmark

http://dx.doi.org/10.1016/j.celrep.2017.03.032

#### SUMMARY

Stem cell-based therapy for type 1 diabetes would benefit from implementation of a cell purification step at the pancreatic endoderm stage. This would increase the safety of the final cell product, allow the establishment of an intermediate-stage stem cell bank, and provide a means for upscaling β cell manufacturing. Comparative gene expression analysis revealed glycoprotein 2 (GP2) as a specific cell surface marker for isolating pancreatic endoderm cells (PECs) from differentiated hESCs and human fetal pancreas. Isolated GP2+ PECs efficiently differentiated into glucose responsive insulin-producing cells in vitro. We found that in vitro PEC proliferation declines due to enhanced expression of the cyclin-dependent kinase (CDK) inhibitors CDKN1A and CDKN2A. However, we identified a time window when reducing CDKN1A or CDKN2A expression increased proliferation and yield of GP2<sup>+</sup> PECs. Altogether, our results contribute tools and concepts toward the isolation and use of PECs as a source for the safe production of hPSC-derived β cells.

#### **INTRODUCTION**

Success in generating human pluripotent stem cell (hPSC)-derived glucose-responsive insulin-producing cells that share functional properties with normal beta cells (Pagliuca et al., 2014; Rezania et al., 2014; Russ et al., 2015) has made the implementation of a cell-based therapy for the treatment of type 1 diabetes a tangible reality. The number of islet cells required for disease recovery has been estimated to be around 300 million to 750 million cells per patient (Bruni et al., 2014; Pagliuca et al., 2014). Thus, to be able to generate a sufficient number of hPSC-derived beta cells to be useful for a large number of

patients, it will be necessary to implement expansion steps. Toward this end, expansion of either undifferentiated hPSCs (Schulz et al., 2012) or proliferative intermediate endodermal progenitors (Cheng et al., 2012; Zhu et al., 2016) has been explored.

During pancreas development, multipotent pancreatic endoderm cells (PECs) with inherent proliferative capacity, co-expressing PDX1, NKX6-1, and SOX9, are responsible for the proper growth of the organ (Kopp et al., 2011; Schaffer et al., 2010; Seymour et al., 2007). The pancreatic epithelium proliferates and expands between embryonic day (E) 8.5 and E11.5 in the mouse (Stanger et al., 2007) corresponding to 25–35 days post-conception in human development (Jennings et al., 2013; Nair and Hebrok, 2015). In contrast to more committed cells with limited to no proliferative capacity, such as the NEUROG3 (NGN3)<sup>+</sup> endocrine progenitors (Castaing et al., 2005), PECs give rise to all mature pancreatic epithelial derivatives, including acinar, ductal, and endocrine cells (Gu et al., 2002; Herrera, 2002; Kawaguchi et al., 2002).

Previous attempts have identified putative markers for human embryonic stem cell (hESC)-derived PECs (CD142) and endocrine cells (CD200/CD318) (Kelly et al., 2011). However, more specific PEC markers remain to be identified, because CD142 labels additional cell types (Kelly et al., 2011).

Proliferation of pancreatic progenitors (both human and mouse) can be induced by co-culture with mesenchymal or endothelial cells (Cheng et al., 2012; Sneddon et al., 2012) or by the addition of mitogenic signals such as fibroblast growth factors (FGFs) or epidermal growth factor (EGF) (Bonfanti et al., 2015; Elghazi et al., 2002; Zhu et al., 2016). However, it remains unclear whether the proliferative capacity of PECs in vitro corresponds to the self-renewal of pancreatic endoderm (PE) that underlies organ growth in vivo (Stanger et al., 2007). Thus, to develop strategies for expanding pure populations of PECs, it is necessary to both improve methods for isolating pure populations of PECs and understand how PEC proliferation is regulated. In this study, we identified glycoprotein 2 (*GP2*) as a specific cell surface marker for the isolation of human PECs from differentiated hESCs and the human fetal pancreas.



<sup>&</sup>lt;sup>2</sup>Lund Stem Cell Center, Department of Laboratory Medicine, Lund University, BMC, B10, 22184 Lund, Sweden

<sup>&</sup>lt;sup>3</sup>Center for Genomic Medicine, Copenhagen University Hospital, Rigshospitalet, Blegdamsvej 9, 2100 Copenhagen, Denmark

<sup>&</sup>lt;sup>4</sup>INSERM U1016, University Paris-Descartes, Cochin Institute, 75014 Paris, France

<sup>&</sup>lt;sup>5</sup>Lead Contact

<sup>\*</sup>Correspondence: semb@sund.ku.dk

Furthermore, we showed that re-plated GP2<sup>+</sup> PECs retain the capacity to differentiate with high efficiency into glucose-responsive insulin-producing beta-like cells. In addition, we discovered that as PECs mature into PDX1<sup>+</sup>/NKX6-1<sup>high</sup> cells in vitro, the expression of the negative cell-cycle regulators *CDKN1a* (also known as p21) and *CDKN2a* (also known as p16) increase. Specifically, we identified a temporal window in which the proliferation and yield of early PDX1<sup>+</sup>/NKX6-1<sup>low</sup> PECs can be enhanced through reduced expression of CDKN1A or CDKN2A. Altogether, our study provides key elements toward a strategy in which isolated GP2<sup>+</sup> PECs can be used as a new source for production of beta cells for future cell replacement therapy in type 1 diabetes.

#### **RESULTS**

# Comparative Gene Expression Analysis of Pancreatic and Posterior Foregut Endoderm

To define the specific gene expression signature of PECs and identify PEC-specific cell surface markers, we first designed a strategy for generating putative PECs (PDX1+/NKX6-1+, protocol A) (Figures 1A and 1B) and posterior foregut endoderm (PFG) cells (PDX1<sup>+</sup>/NKX6-1<sup>-</sup>, protocol B) (Figures 1A and 1E). Analysis of the gene expression pattern of known pancreatic endoderm markers in PDX1+ and PDX1- cells (GFP+ and GFP- cells using a PDX1-EGFP hESC reporter [PDXeG]) (Figures S1A-S1F) demonstrated that PDX1, CDH1, ONECUT1, and SOX9 were all significantly upregulated in the GFP+ cells generated by both protocols (Figures 1C, 1D, 1F, and 1G). However, while protocol A generated GFP+ cells with significant PDX1, NKX6-1, and MNX1 upregulation, the GFP+/PDX1+ cells from protocol B expressed lower levels of NKX6-1 and MNX1 (Figures 1D and 1G). Immunostainings at day 17 confirmed the expression of NKX6-1, SOX9, CDH1, and HES1 in the pancreatic endoderm cells obtained with protocol A (Figure S1G; data not shown). Collectively, these results suggest that the GFP+ cells obtained with protocol A represent bona fide PECs, while GFP+ cells obtained with protocol B correspond to PFG cells.

# Identification of Cell Surface Markers for Prospective Isolation of PECs

To identify PEC-specific cell surface markers, we performed microarray analysis to compare the gene expression pattern in PDX1<sup>+</sup>/NKX6-1<sup>+</sup> (GFP<sup>+</sup> PECs), PDX1<sup>+</sup>/NKX6-1<sup>-</sup> (GFP<sup>+</sup> PFG), and PDX1- (GFP-) cells (Figure 2A). Only genes with a fold change above 1.4 (p < 0.005) were selected for further analysis. A total of 3,403 genes (3,791 probe sets) were differentially expressed among the three sample groups. Hierarchical clustering revealed 382 genes enriched in PECs compared to PFG cells, while 698 genes were enriched in the PECs compared to GFP- cells. Interestingly, 115 genes were specifically enriched in PECs compared to PFG and GFP- cells (Figure 2B; Table S1). Gene ontology analysis showed that processes related to proliferation (e.g., cell cycle, epithelial cell proliferation, ad DNA replication) were significantly enriched in the PDX1+/NKX6-1+ PECs (Figure 2C). Consistent with our initial analysis, genes that are induced early during pancreatic endoderm specification, such as *PDX1*, *HHEX*, *GATA4*, and *FOXA2*, were present in both PECs and PFG cells, while markers of late PECs, such as *NKX6-1*, *SOX9*, *ONECUT1/2*, and *PRDM16*, were specifically enriched in the PEC population (Figure 2D). *CD142* (also known as *F3*) and *CD200*, two cell surface markers previously shown to enrich for pancreatic endoderm cells and endocrine progenitors (Kelly et al., 2011), were expressed in both PECs and PFG cells (Figure 2D).

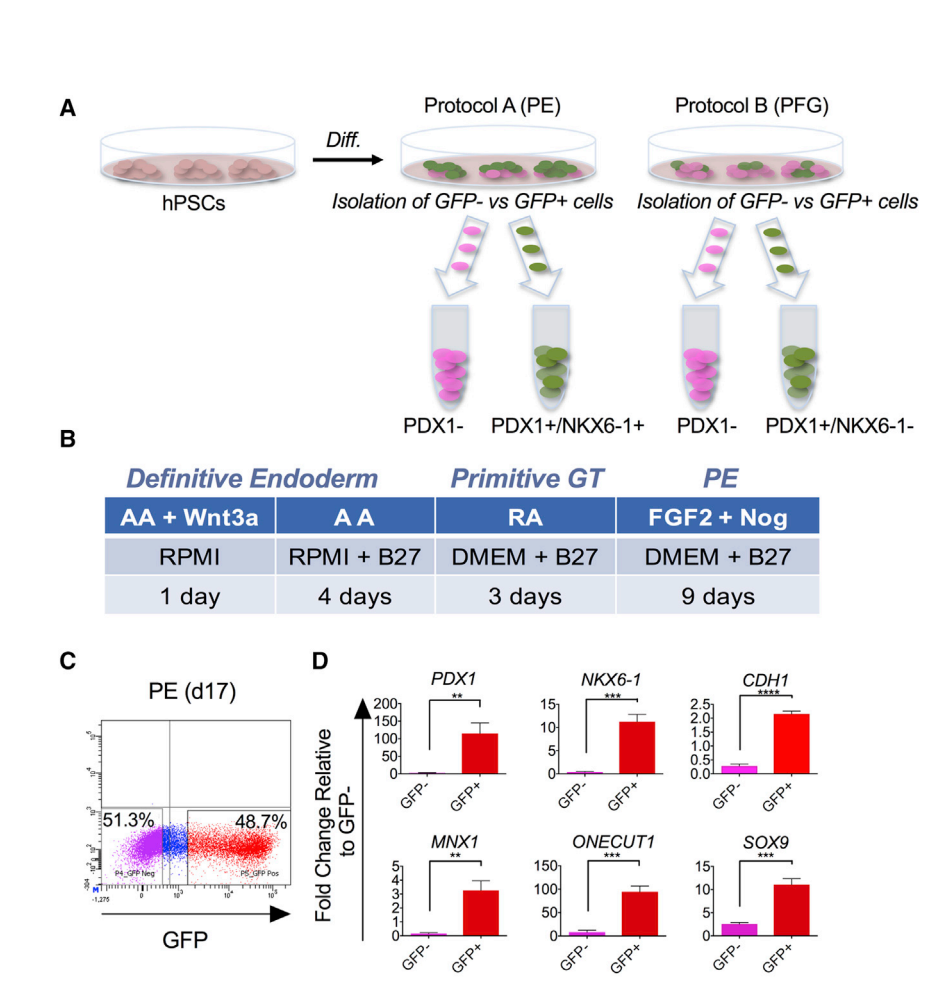
For a more in-depth analysis, nine sub-clusters were created by hierarchical clustering. Sub-cluster 3a represents genes enriched in the GFP- cells, including the mesenchymal markers GATA2, MEIS2, TBX2, EYA1, FGFR1, HEY2, HOXA2, and VIM. Genes enriched in both PECs and PFG cells were confined to sub-cluster 6-PDX1, CDH1, GATA4, HNF1a, F3, EPCAM, FOXA2, and HES-whereas pancreatic endoderm-associated genes in sub-cluster 5, such as NKX6-2, SOX9, EGFR, ERBB2, and ONECUT2, were upregulated in PECs (Figure 2E). We identified cell surface makers that could potentially be used for the isolation of PECs. Specifically, glycoprotein 2 (zymogen granule membrane GP2) was enriched in PDX1+/NKX6-1+ PECs (subcluster 5), Folic receptor 1 (FOLR1) was enriched in all PDX1+ cells (sub-cluster 6), and Integrin alpha 4 (ITGA4 or CD49d) was enriched in GFP<sup>-</sup> cells (sub-cluster 3a) (Figure 2E). Overall, our expression analysis not only reveals a set of genes uniquely expressed in PECs but also provides putative cell surface markers for isolation of PECs.

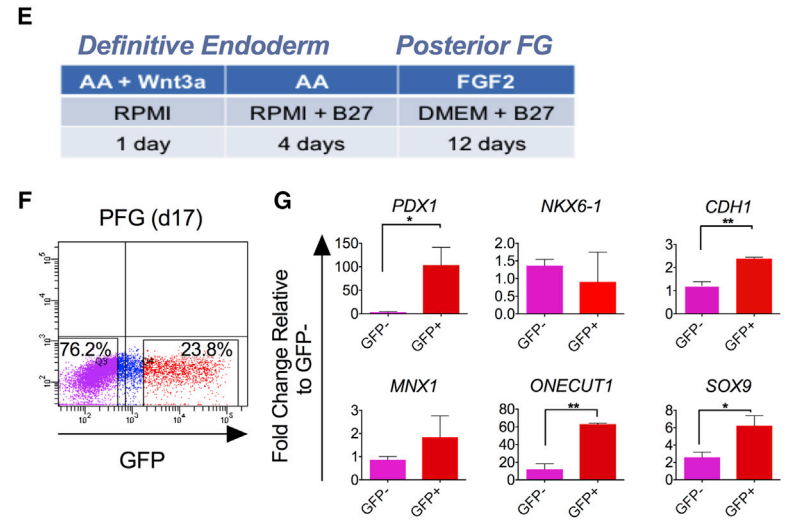
### **Functional Validation of Identified Cell Surface Markers**

To validate GP2, FOLR1, and ITGA4 for the isolation of PECs, flow cytometry analysis of differentiated PDXeG cells was carried out (Figure 3A). Double staining with antibodies against GP2 and ITGA4 showed that most GFP+ cells (76%) co-expressed GP2, while 71% of the GFP- cells expressed CD49d at day 17. Only a low fraction of the GFP $^-$  cells (3%) expressed GP2, and basically none (1%) of the GFP+ cells expressed ITGA4 (Figure 3A). To confirm GP2's specificity in labeling the PDX1<sup>+</sup>/NKX6-1<sup>+</sup> cells, gene expression analysis on sorted cell fractions (ITGA4+/GP2-, ITGA4-/GP2+, and GFP+/GP2-) was performed. This analysis revealed that the pancreas-associated markers PDX1, NKX6-1, MNX1, SOX9, FOXA2, and ONECUT1 were all significantly enriched in the ITGA4<sup>-</sup>/GP2<sup>+</sup> cells compared to the ITGA4+/GP2- cells. Furthermore, while similar levels of PDX1, SOX9, FOXA2, and ONECUT1 were expressed in GFP<sup>+</sup>/GP2<sup>-</sup> and ITGA4<sup>-</sup>/GP2<sup>+</sup> cells, NKX6-1 and MNX1 were exclusively enriched in ITGA4-/GP2+ cells (Figure 3B). As expected, both GP2 and FOLR1 were enriched in the ITGA4-/ GP2+ cells, whereas ITGA4 was enriched in the ITGA4+/GP2cells (Figure S2A). Similar results were obtained from the gene expression analysis performed on the cell fractions stained with FOLR1 and ITGA4 (Figures S2B and S2C). Altogether, these results suggest that GP2 and FOLR1 represent specific markers for PECs.

Next, we confirmed the cell surface markers in genetically unmodified hESCs under feeder-free conditions. This adaptation resulted in few ITGA4<sup>+</sup> cells (Figure 3C; Figure S2E). Consistent with the previous results, the pancreatic markers *PDX1*, *NKX6-1*, *SOX9*, *ONECUT1*, *FOXA2*, and *MNX1* were all significantly enriched in ITGA4<sup>-</sup>/GP2<sup>+</sup> cells in comparison







to ITGA4+/GP2- and ITGA4-/GP2- cells (Figure 3D). PDX1 expression was still detectable in the ITGA4-/GP2- cells; however, these cells expressed low levels of NKX6-1 (Figure 3D) and GP2 (Figure S2D), suggesting that these cells most likely represent PDX1+ PFG cells. Consistently, FOLR1 was also expressed in the ITGA4-/GP2- cell fraction (Figure S2F). Moreover, although pancreatic markers were enriched in the

#### Figure 1. Analysis of In Vitro Differentiated PDXeG hESCs

(A) Two differentiation protocols were used to obtain either pancreatic endoderm cells co-expressing PDX1 and NKX6-1 (protocol A, PEC) or posterior foregut cells expressing PDX1 but lacking NKX6-1 (protocol B, PFG).

(B) Schematic depicting the differentiation protocol referred to as protocol A, generating PECs.

(C) FACS isolation of GFP+ and GFP- fractions at day 17 in hESCs treated according to protocol A. (D) Gene expression analysis of sorted GFP+ and GFP cells showed significant enrichment of PE markers (importantly PDX1 and NKX6-1) in the GFP+ cells. The graphs depict mean expression ± SEM (n = 5) and represent the fold increase compared to control samples (GFP- cells) at day 17. The control sample was arbitrarily set to a value of one. \*\* $p \le 0.01$ , \*\*\* $p \le 0.001$ , \*\*\*\* $p \le 0.0001$ . (E) Schematic depicting the differentiation protocol referred to as protocol B, generating PFG cells. (F) FACS isolation of GFP+ and GFP- cells (from day 17) obtained by protocol B.

(G) Gene expression analysis of sorted GFP+ and GFP- cells showed that whereas markers such as PDX1, CDH1, ONECUT1, and SOX9 were enriched in the GFP+ cells, neither NKX6-1 nor MNX1 was significantly upregulated in the GFP+ cells. The graphs depict mean expression  $\pm$  SEM (n = 2-4) and represent the fold increase compared to control samples (GFP<sup>-</sup> cells) at day 17. \*p  $\leq$  0.05, \*\* $p \le 0.01$ .

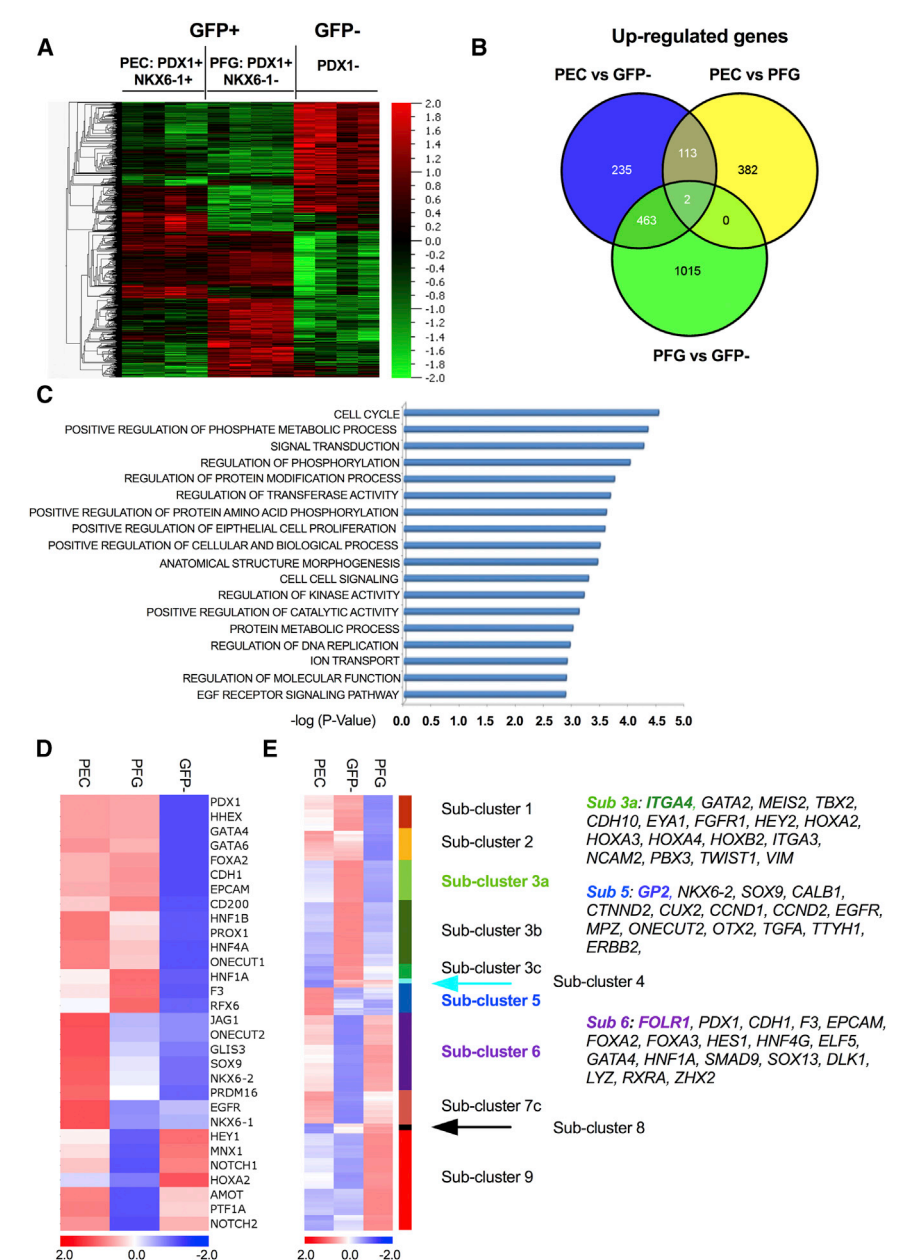
See also Figure S1.

ITGA4<sup>-</sup>/FOLR1<sup>+</sup> cells, ITGA4<sup>-</sup>/FOLR1<sup>-</sup> cells still expressed PDX1, NKX6-1, and GP2 (Figure S2F). These data underscore that while GP2 is highly specific for hPSC-derived PDX1+/NKX6-1+ PECs, FOLR1 recognizes both PECs and PFG cells.

#### **GP2 Enables Isolation of Bona Fide PECs from Human Fetal Pancreas**

To corroborate the relevance of GP2 as a specific PEC marker, we examined the expression of GP2 and ITGA4 in human fetal pancreas at 9.1 weeks in development. Consistent with differentiated hESCs, GP2 and ITGA4 showed no overlap in the human fetal pancreas (Figure 3E). While ITGA4 is expressed in the mesenchyme, GP2 is confined to the

epithelium (data not shown). qPCR analysis showed that GP2+ cells are significantly enriched for PDX1 and NKX6-1 (Figure 3F). PDX1 and NKX6-1 co-expression was confirmed in the GP2+ cells by flow cytometry (Figure 3G). Collectively, our results demonstrate that GP2 can be used for isolation of PDX1+/ NKX6-1+ PECs from heterogeneous populations of differentiated hPSCs, as well as from human fetal pancreas in vivo.



# Validation of GP2 Using an Independent Differentiation **Protocol**

To further substantiate the ability of GP2 to specifically recognize PECs, we used a slightly modified version of a published feederfree differentiation protocol (Figure 4A) (Rezania et al., 2013). This protocol generates a more heterogeneous cell population with less GP2+ cells (Figure 4B) in comparison to our modified protocol (Figures S4A and S5B). Consistent with the results shown earlier, GP2+/GFP+ cells expressed high levels of the PEC-associated genes PDX1, NKX6-1, SOX9, and GP2 (Figure 4C). FOLR1 expression was detected in all sorted populations (GP2-/GFP-, GP2-/GFP+, and GP2+/GFP+ cells), highlighting again that GP2 is a more specific marker for PECs

#### Figure 2. Global Gene Expression Analysis of In Vitro-Derived PDX1+/NKX6-1+ PECs versus PDX1+/NKX6-1 - Cells

(A) Heatmap displaying hierarchical clustering of genes differentially expressed in the PDX1+/ NKX6-1+ (PEC, GFP+) pancreatic progenitors generated using protocol A, PDX1+/NKX6-1- (PFG, GFP+) posterior foregut cells generated using protocol B, and PDX1<sup>-</sup> (GFP<sup>-</sup>) cells from protocol A. (B) Venn diagrams showing the distribution of genes upregulated in PECs versus GFP cells, PECs versus PFG cells, and PFG cells versus GFP<sup>-</sup> cells at day 17.

- (C) Gene ontology (GO) analysis showing enrichment of genes in the PDX1+/NKX6-1+ pancreatic endoderm cells. Representative GO categories are shown and plotted against -log (p value).
- (D) Expression of common genes expressed in the PFG and PE was analyzed in the different sub-
- (E) Hierarchical clustering of the genes differentially expressed in the three-comparison analysis depicted in (A) (average expression levels are shown). The bars indicate sub-clusters with relevant genes; nine sub-clusters were created. Subcluster 3a shows genes enriched in the GFP- cell population, including the cell surface marker CD49d (ITGA4), whereas sub-cluster 5 displays genes enriched in the pancreatic endoderm cells (PEC cell fraction), also including the cell surface marker GP2. Sub-cluster 6 indicates genes enriched in PDX1+ cells irrespective of NKX6-1 expression (PFG cells and PECs), such as CDH1 (ECAD), EPCAM, F3 (CD142), and the cell surface marker FOLR1.

See also Table S1.

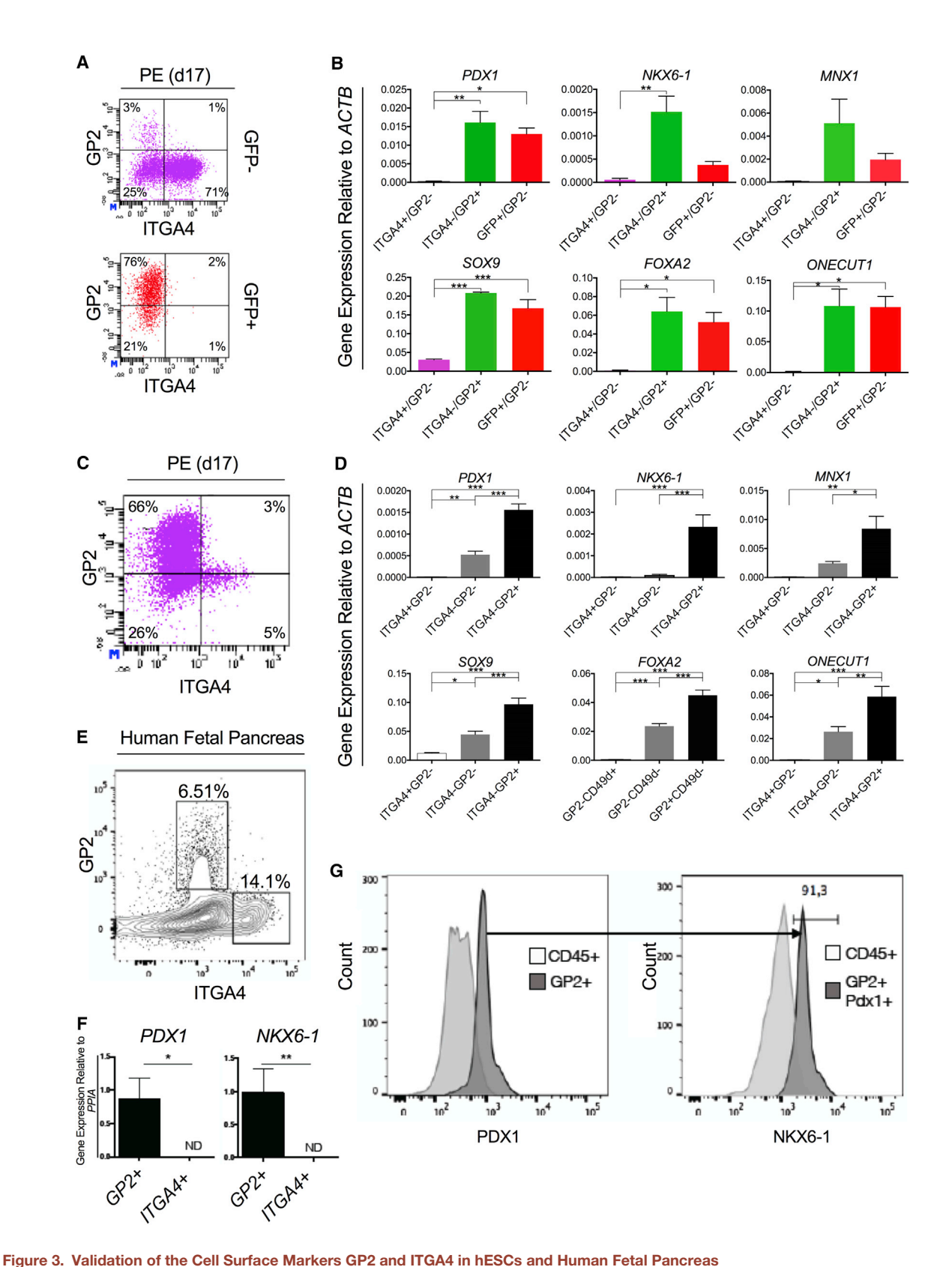
compared to FOLR1 (Figure 4C). As expected, the highest level of ITGA4 was expressed in the GP2-/GFP- cells (Figure 4C). GP2-mediated enrichment of PECs was confirmed at the protein level by co-staining the different cell fractions with antibodies against PDX1 and NKX6-1 (Figure 4D). Finally, independent quantification analysis showed a similar percentage of GP2+ and PDX1+/ NKX6-1+ cells at the PE stage (14.8%

GP2+ cells versus 15% PECs) (Figures 4E-4G). In sum, these results unambiguously show that GP2 specifically labels PDX1+/ NKX6-1+ PECs.

# Comparative Analysis of GP2 with CD142 and CD200

Analysis of the expression pattern of the previously reported cell surface markers CD142, CD200, and CD318 (Kelly et al., 2011) revealed that CD318 was significantly enriched in the PDX1<sup>-</sup>/ GFP<sup>-</sup> cells (data not shown), while CD142 and CD200 were present on both PDX1<sup>+</sup>/GFP<sup>+</sup> and PDX1<sup>-</sup>/GFP<sup>-</sup> cells (Figure S3A). Comparative analysis of GP2, CD142, and CD200 stainings revealed that CD142 and CD200 labeled most differentiated cells, while GP2 only stained a subset of the cells (Figures S3A-S3C).





(A) Flow cytometry analysis of the cell surface markers GP2 and ITGA4 performed on differentiated hESCs cultured on MEFs (day 17), confirmed that GP2 was highly expressed in the GFP<sup>+</sup> cells, whereas ITGA4 was enriched in the GFP<sup>-</sup> cells.

qPCR analysis of the sorted cell populations showed an enrichment of the PE-specific genes PDX1, NKX6-1, and SOX9 in GP2+ cells compared to CD142+ and CD200+ cells (Figure S3D). Furthermore, immunostainings of the CD142<sup>+</sup> and CD200<sup>+</sup> cell fractions with PDX1 and NKX6-1 antibodies unequivocally showed that GP2 is superior in labeling PDX1+/NKX6-1+ PECs (Figure 4D; Figure S3E). Altogether, our findings demonstrate that GP2 specifically labels PDX1+/NKX6-1+ PECs and can be used for purification of PECs from heterogeneous populations of differentiated hPSCs independent of culture system or differentiation protocol.

#### Lineage Potential of GP2<sup>+</sup> PECs toward Beta Cells

To assess the ability of isolated GP2+ PECs to differentiate into mono-hormonal insulin-producing beta-like cells, we optimized our differentiation protocol depicted in Figure 1B to generate glucose-responsive beta-like cells (protocol C) (Figure S4A). Specifically, two more stages were introduced in which the cells were first differentiated in the presence of TPB and Noggin and finally in a medium containing forskolin, ALK5i, Noggin, and nicotinamide. This protocol generated on average 60%-80% PDX1+/ NKX6-1<sup>+</sup> PECs at the PE stage (days 17-18) (Figures S4B and S4C). This percentage can be directly correlated with the number of GP2<sup>High</sup> cells present in the culture (Figure S4D). Furthermore, we have observed that the GP2<sup>Low</sup> cell population shifts into a GP2<sup>High</sup> cell population over time (data not shown) and that this shift correlates with the increase in NKX6-1 expression. This suggests that the GP2<sup>High</sup> cells are late PECs (co-expressing PDX1 and NKX6-1), whereas GP2<sup>Low</sup> cells are early PECs in which NKX6-1 expression is just initiated. As the cells are differentiated further, INS and GLU gene expression is observed from day 23 onward (Figure S4E). On day 32, glucose-responsive C-peptide (CPEP+) cells that were also positive for PDX1 and for NKX6-1 were detected, while few glucagon (GLU+) cells (3.6%) were observed (Figures S4F-S4H; see also Figure 5G).

GP2+ PECs sorted on day 18 were re-plated in the same differentiation medium for 2 weeks (Figures 5A and 5B). Negative selection with ITGA4 was not necessary, because extremely few ITGA4<sup>+</sup> cells appeared (Figure 5C). While CPEP<sup>+</sup> cells emerged from both GP2<sup>High</sup> cells and GP2<sup>Low</sup> cells, there was a significant enrichment of CPEP+ cells from the GP2High cells (44% from GP2<sup>High</sup> versus 18% from GP2<sup>Low</sup>) (Figures 5D and 5E). Similar to the unsorted cultures, few GLU+ cells were observed, although GP2+ purification at the PE stage resulted in an enrichment of GLU<sup>+</sup> cells (8.3% versus 3.2%) (Figure 5G). Furthermore, most mono-hormonal CPEP+ cells co-expressed PDX1, and CPEP+/NKX6-1+ cells were observed (Figure 5F). Insulin secretion analysis of the CPEP+ cells derived from GP2High cells revealed an approximately 2-fold increase in insulin release in response to high versus low glucose (Figure 5H). This result corresponds to the behavior of CPEP+ cells derived in unsorted cultures (Figure S4H). The level of glucose responsiveness is comparable to what has been previously published (Pagliuca et al., 2014; Rezania et al., 2014). Thus, we have developed an experimental system for generating glucose-responsive monohormonal CPEP+ cells from isolated hPSC-derived GP2+ PECs.

These experiments were repeated on the good manufacturing practice (GMP)-graded hESC line MShef-7 (Figure 6). Similar to the HUES4 cell line, INS and GLU expression was detected from day 23 and onward (Figure 6A) and ITGA4+ cells were scarce at day 17 (Figure 6B).

Generation of CPEP+ cells was in general less efficient in MShef-7 cultures compared to HUES4 (Figure 6C). However, sorted and re-plated GP2High MShef-7 cells generated significantly higher numbers of CPEP+ cells compared to unsorted and GP2<sup>Low</sup> cells (Figures 6D-6F; Figures S5C and S5D). Slightly more GLU+ cells were observed with the MShef-7 cell line in comparison to the HUES4 cell line (5.0% versus 3.2%), and analogous to the HUES4 cultures, GP2+ purification resulted in an enrichment of GLU<sup>+</sup> cells (11.1% versus 8.3%) (Figure 6G), Similarly, most CPEP+ cells were mono-hormonal, and PDX1 and CPEP+/NKX6-1+ co-expressing cells were observed (Figures S5D and S6E). The CPEP+ cells derived from the GP2High cells were also glucose responsive (Figure 6H). Altogether, these results substantiate the use of GP2 in isolating PECs with the capacity to differentiate into beta-like cells.

# Silencing of CDKN1A or CDKN2A Promotes Cell-Cycle Progression of GP2<sup>+</sup> PECs

Current differentiation protocols of insulin-producing beta-like cells from hPSCs do not support significant expansion of PECs, suggesting that PEC proliferation is inhibited in vitro. Directed differentiation of hESCs toward pancreatic endoderm is associated with a decrease in proliferation (Figure S6A). Although MKI67 expression is maintained until day 11, it drops concomitant with increased expression of PDX1 and NKX6-1 (Figures S6A and S6B). Consistently, microarray analysis revealed that the negative cell-cycle regulators CDKN1A (p21)

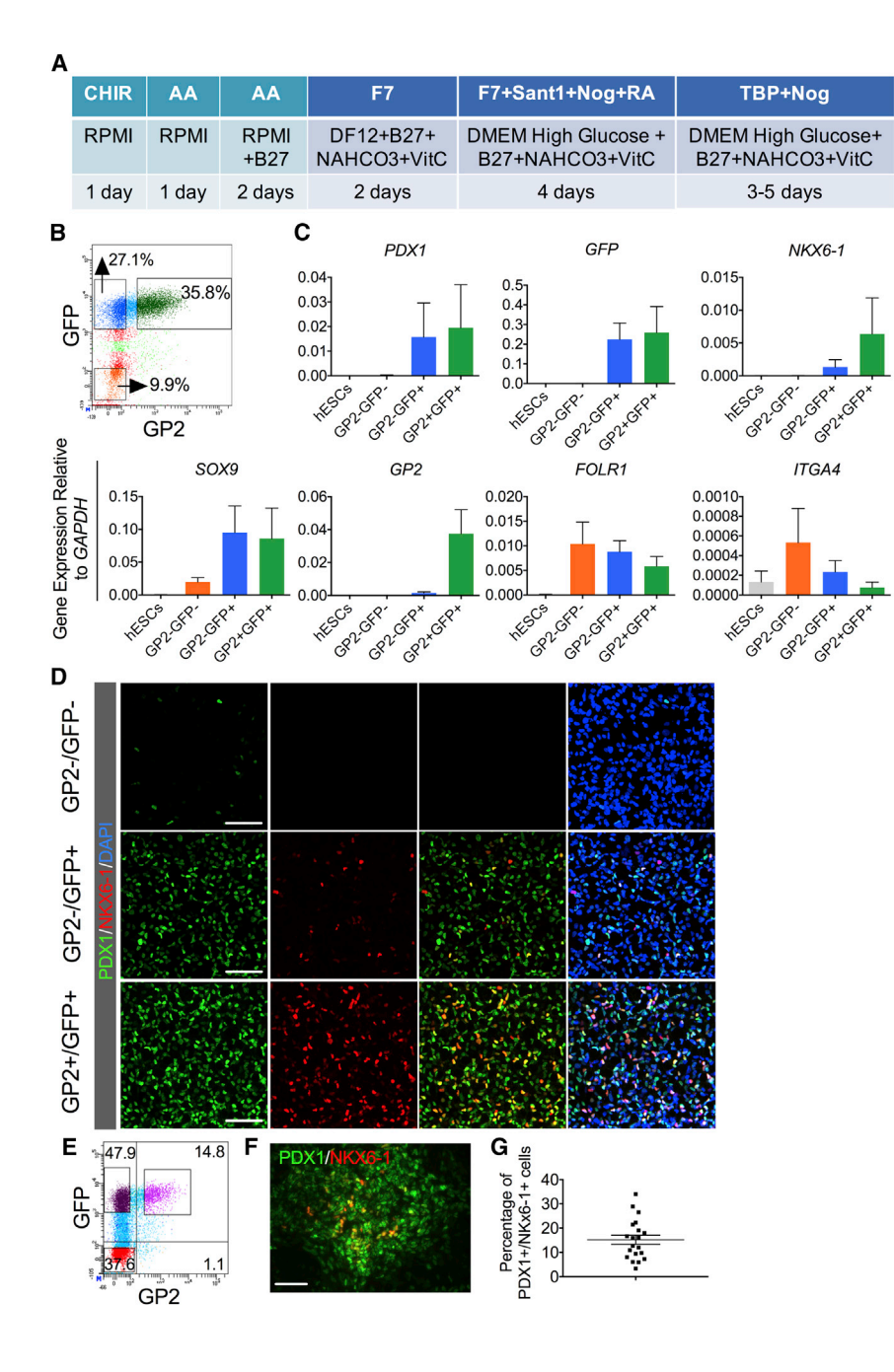
<sup>(</sup>B) Gene expression analysis showed that PE markers were highly enriched in GP2+/ITGA4- sorted cells. The data are shown as mean expression ± SEM (n = 3). \* $p \le 0.05$ , \*\* $p \le 0.01$ , \*\*\* $p \le 0.001$ .

<sup>(</sup>C) Flow cytometry analysis of GP2 and ITGA4 in genetically untagged HUES4 cells, cultured in a feeder-free system using protocol A depicted in Figure 1. (D) GP2\*ITGA4\*, ITGA4\*GP2\*, and GP2\*ITGA4\* cells were sorted and the gene expression pattern was analyzed. PDX1, SOX9, MNX1, and NKX6-1 were significantly enriched in the GP2+ITGA4<sup>-</sup> cell fractions. The remaining PDX1+ cells in the GP2-ITGA4- fraction express only low levels of NKX6-1, confirming that GP2 specifically enrich for  $PDX1^+/NKX6-1^+$  cells. The data are shown as mean expression  $\pm$  SEM (n = 5-6). \*p  $\leq$  0.05, \*\*p  $\leq$  0.01, \*\*\*p  $\leq$  0.001, \*\*\*\*p  $\leq$  0.0001. (E) Flow cytometry analysis of GP2 and ITGA4 expression in human fetal pancreas (9.1 weeks in development [WD]) gated on non-hematopoietic and nonendothelial cells (CD45<sup>-</sup>CD31<sup>-</sup>).

<sup>(</sup>F) qPCR analysis of PDX1, and NKX6-1 expression in FACS-sorted GP2+ and ITGA4 cell populations, showed significant enrichment of PDX1 and NKX6-1 in the GP2+ versus the ITGA4 cells. Results are shown as mean expression ± SD, presented in arbitrary units (AU) relative to expression of the control gene PPIA. \*p = 0.023, \*\*p = 0.010. ND, non-detected.

<sup>(</sup>G) Flow cytometry analysis of PDX1 and NKX6-1 expression in GP2<sup>+</sup> and CD45<sup>+</sup>/CD31<sup>+</sup> cells at 8.7 WD. 91% of the GP2<sup>+</sup>/PDX1<sup>+</sup> cells co-expressed NKX6-1. CD45<sup>+</sup>CD31<sup>+</sup> cells were used as a negative control for PDX1 and NKX6-1 expression. FACS plots are representative of three independent experiments. See also Figure S2.





and CDKN2A (p16) were specifically enriched in the PDX1+/ NKX6-1<sup>+</sup> PECs at day 17 (Figure S6D). Further analysis revealed that the expression of both CDKN1A and CDKN2A increased at day 14 and remained high during subsequent differentiation stages (Figure S6A). Both CDKN1A and CDKN2A block cell-cycle progression by inhibiting the activity of the cyclin/cyclindependent kinase (CDK) complexes that regulate progression through the cell cycle (Figure S6C) (Besson et al., 2008). To test whether increased expression of CDKN1A and CDKN2A were responsible for the drop in PEC proliferation, differentiated hESCs corresponding to PDX1+/NKX6-1+ late PECs (day 17) were re-seeded and transfected with small interfering RNA

Figure 4. Validation of GP2 Using an Independent and Previously Published Differentiation Protocol

(A) Scheme for generation of hPSC-derived PECs according to a modified protocol by Rezania et al. (2013). AA, Activin A; F7, FGF7; Nog, Noggin; DF12, DMEMF12; VitC, vitamin C.

(B) Characterization of GFP and GP2 expression by flow cytometry on differentiated PDXeG cells.

(C) qPCR analysis of the sorted populations: GP2-GFP-, GP2-GFP+, and GP2+GFP+ cells showed that NKX6-1 expression is significantly enriched in the GP2+GFP+ cell fraction in comparison to the GP2<sup>-</sup>GFP<sup>+</sup> cell fraction. The data are shown as mean expression  $\pm$  SEM (n = 3).

(D) Immunofluorescence stainings of the sorted cell populations confirmed significant enrichment of PDX1+/NKX6-1+ cells in the GP2+/GFP+ cells. Scale bars, 100 um.

(E) Flow cytometry analysis of differentiated PDXeG cells on day 13.

(F) PDX1 and NKX6-1 expression in cultures at day 13 was analyzed by immunofluorescence. Scale bars. 100 μm.

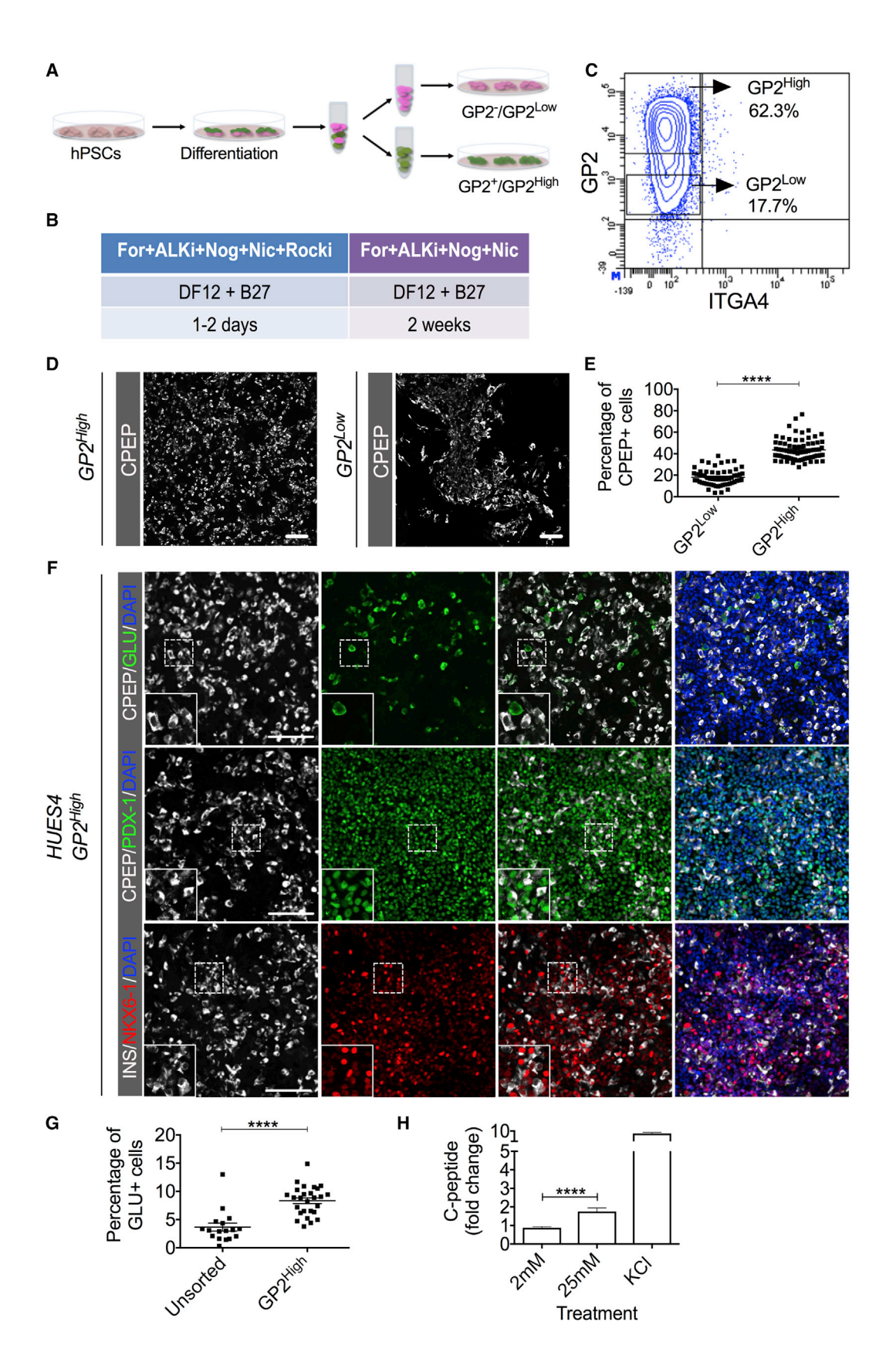
(G) Percentage of PDX1+/NKX6-1+ quantified from day 13 cultures.

See also Figure S3.

(siRNA) against CDKN1A or CDKN2A. Knockdown efficiency was assessed by gPCR analysis 24 hr after the transfection (Figures S6E and S6F). Unexpectedly, knocking down either CDKN1A or CDKN2A had no significant impact on 5-ethynyl-2'-deoxyuridine (EdU) incorporation (Figures S6G-S6I) and MKI67 expression (Figures S6J and S6K). We confirmed that downregulation CDKN1A or CDKN2A expression had no negative influence on the differentiation of the PECs, because PDX1 and NKX6-1 expression was comparable to scrambled controls (Figure S6L).

To examine whether blocking the increased expression of CDKN1A and CDKN2A at an earlier time point would increase PEC proliferation, we repeated the

knockdown experiments at day 11. Knockdown efficiency was confirmed by qPCR and western blot analysis 24 hr after transfection (Figures S7A-S7C). In contrast to experiments performed at day 17, this time we observed that reduced expression of CDKN1A and CDKN2A resulted in increased number of cells in the G2/M and S phases of the cell cycle, respectively (Figures 7A-7C). qPCR analysis confirmed that MKI67 expression increased 24 hr after knockdown of CDKN1A, but not CDKN2A (Figures 7D and 7J). Nevertheless, we observed a significant increase in the number of MKI67+ cells (Figures 6E, 6F, 6K, and 6L), as well as in the number of PDX1+/NKX6-1+ PECs 72 hr after transfection (Figures S7D and S7E). This increase correlated with





an increase in the total number of cells (Figure S7F). Altogether, these results suggest that preventing increased expression of CDKN1A or CDKN2A in early hESC-derived PDX1+/NKX6-1Low PECs enhances their proliferative capacity.

To address whether the CDK inhibitors autonomously affect PEC proliferation, we knocked down the expression of CDKN1A and CDKN2A and subsequently assessed the outcome on the proliferative capacity of GP2+ PECs specifically. Consistent with the results from the unsorted cell population, knockdown of CDKN1A and CDKN2A increased the number of GP2+ PECs that transitioned into the G2/M and S phases of the cell cycle, respectively (Figures S7G-S7K). Altogether, by preventing increased expression of CDKN1A and CDKN2A in early hPSCderived PECs, the proliferative capacity of PECs can be enhanced during in vitro differentiation (Figure 7M).

#### **DISCUSSION**

In this study, we report the identification of a cell surface marker, GP2, for efficient purification of human PDX1+/NKX6-1+ PECs endowed with the capacity to give rise to glucose-responsive insulin-producing beta-like cells. Furthermore, by counteracting the increased expression of the cell-cycle inhibitors CDKN1A and CDKN2A in the early PECs, the proliferative capacity of hPSC-derived PECs can be sustained in vitro.

The unique experimental design to compare the gene expression pattern in isolated PFG cells and PECs allowed us for to identify 115 genes exclusively enriched within human PECs (Table S1). Comparing our PE gene list with another study, which systematically analyzed genes expressed in heterogeneous cell populations at intermediate pancreatic differentiation stages (Xie et al., 2013), showed that 16 (including GP2) of our 115 genes overlapped with their "PE genes" (Table S2). This gene signature of human PE provides a unique source for interrogating unanswered questions in PE biology, such as the molecular machinery involved in PEC maturation (increased expression of NKX6-1) and self-renewal.

Our genome-wide expression analysis showed enrichment of the integral membrane protein GP2 in the PDX1<sup>+</sup>/NKX6-1<sup>+</sup> PECs. GP2 expression has previously been described in the acinar cells in the human adult pancreas (Hoops and Rindler, 1991; Yu et al., 2004) (http://www.proteinatlas.org/) but the role and function of GP2 during pancreas development has not been examined. Hence, we show that GP2 is expressed in the human PECs and that it can be used as a cell surface marker for isolation of

PECs. Furthermore, a comparison between GP2 and previously published markers CD142 and CD200 (Kelly et al., 2011) demonstrated the superiority of GP2 in labeling PDX1<sup>+</sup>/NKX6-1<sup>+</sup> PECs both in heterogeneous populations of differentiated hESCs and in human fetal pancreas. In addition, the broad applicability of GP2 as a cell surface marker for isolation of PECs was proved by using independent differentiation protocols and cell lines.

During development, proliferation of pancreatic progenitor cells is promoted by factors secreted by the surrounding mesenchymal tissue (Attali et al., 2007; Bhushan et al., 2001; Ye et al., 2005). Co-culture of pancreatic endoderm and mesenchymal cells promote expansion of the PDX1+ population while maintaining its progenitor identity. These activities are mediated partly by FGF10 and EGF signaling (Attali et al., 2007; Bonfanti et al., 2015; Guo et al., 2013; Zhang et al., 2009). However, the underlying mechanism for how these factors promote pancreatic progenitor proliferation has not been elucidated. Here, we identify the cell-cycle inhibitors CDKN1A and CDKN2A as relevant regulators of PEC proliferation during in vitro differentiation. We show that increased expression of PDX1 and NKX6-1, a hallmark of late PECs, coincides with increased expression of CDKN1A and CDKN2A and a significant decrease in the proliferative capacity of PECs. Moreover, our observation that lowered expression of CDKN1A and CDKN2A sustains proliferation of early PECs is consistent with previous work linking repression of CDKN1A and CDKN2A activities to self-renewal and expansion of other stem cell or progenitor populations (Kippin et al., 2005; Koike et al., 2014; Orford and Scadden, 2008).

Although reduction of both CDKN1A and CDKN2A levels promotes an overall increase in proliferation of early PECs, their effect on cell-cycle progression, as well as the immediate impact on MKI67 expression, differs, suggesting different mechanisms of action. CDKN1A and CDKN2A belong to different families of CDK inhibitors. CDKN1A is a member of the Cip/Kip family and binds to multiple Cdk-cyclin complexes, inhibiting their catalytic activities at the G<sub>1</sub>/S- and G<sub>2</sub>/M-phase checkpoints. CDKN2A belongs to the INK4 family and blocks entry into the S phase by targeting the CDK4/6-cyclin complexes that are present in G1 phase (Figure S6C) (Besson et al., 2008; Donovan and Slingerland, 2000; Yoon et al., 2012). It is possible that the activation of a broader range of Cdk-cyclin complexes upon reduction of CDKN1A levels results in a faster progression through the cell cycle compared to the CDKN2A knockdown. This may explain the observed differences in the number of cells in the G<sub>2</sub>/M and S phases. This notion could also explain the lack of immediate

#### Figure 5. Differentiation of Purified GP2+/ITGA4 - PECs into Glucose-Responsive Insulin-Expressing Cells

(A) Schematic illustrating differentiation of hESCs into PECs that are dissociated and stained with the cell surface markers ITGA4 and GP2.

(B) Table depicting the differentiation protocol to generate insulin-expressing cells from PECs. Rocki is omitted when the protocol is applied to unsorted cultures. Rocki, Rock inhibitor; For, forskolin; Alki, Alk5 inhibitor; Nog, Noggin; Nic, nicotinamide; DF12, DMEM/F-12; B27, B27 supplement.

- (C) Flow cytometry analysis of differentiated PECs (from day 18) stained with GP2 and ITGA4.
- (D) C-peptide staining of re-plated GP2<sup>High</sup>- and GP2<sup>Low</sup>-expressing cells. Scale bars, 100 μm.
- (E) Percentage of CPEP+ cells in the GP2+High and GP2Low cells is shown. \*\*\*\* $p \le 0.0001$ .
- (F) Immunofluorescence analysis of FACS-sorted GP2+/ITGA4- pancreatic endoderm cells re-plated and differentiated to insulin-expressing cells. Scale bars, 100 μm.
- (G) Percentage of GLU<sup>+</sup> cells in the unsorted and GP2<sup>High</sup> cells is shown. \*\*\*\*p ≤ 0.0001.
- (H) The release of human C-peptide was measured in the differentiated GP2+/ITGA4- cells by a static glucose-stimulated insulin secretion assay (GSIS). Error bars represent mean expression  $\pm$  SEM (n = 4), \*\*\* p  $\leq$  0.001, and \*\*\*\* p  $\leq$  0.0001. See also Figure S4.

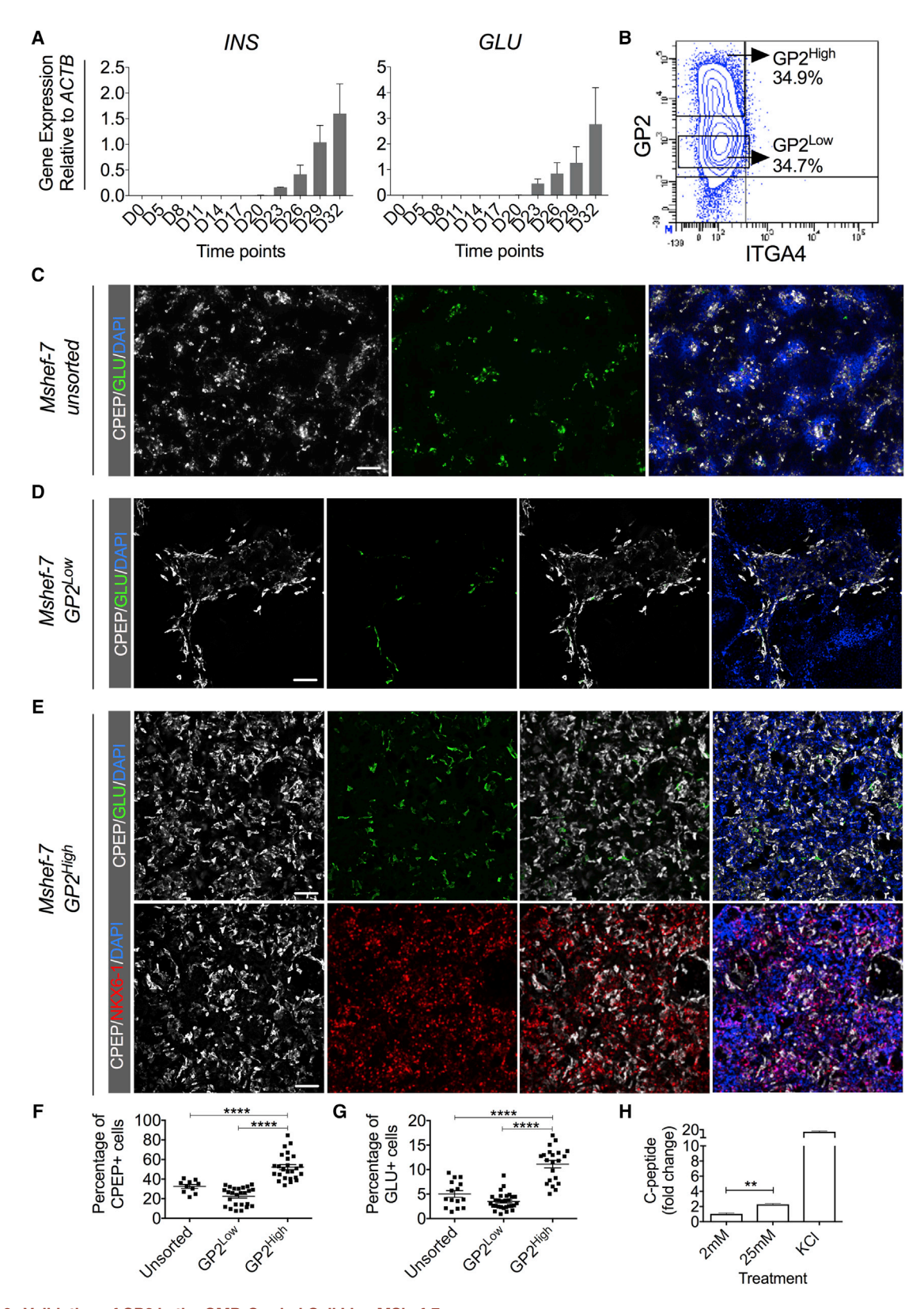


Figure 6. Validation of GP2 in the GMP-Graded Cell Line MShef-7
(A) Time course analysis of *INS* and *GLU* expression in differentiated MShef-7 cells. The data are shown as mean expression ± SEM (n = 3).
(B) Flow cytometry analysis of differentiated PECs stained with GP2 and ITGA4.



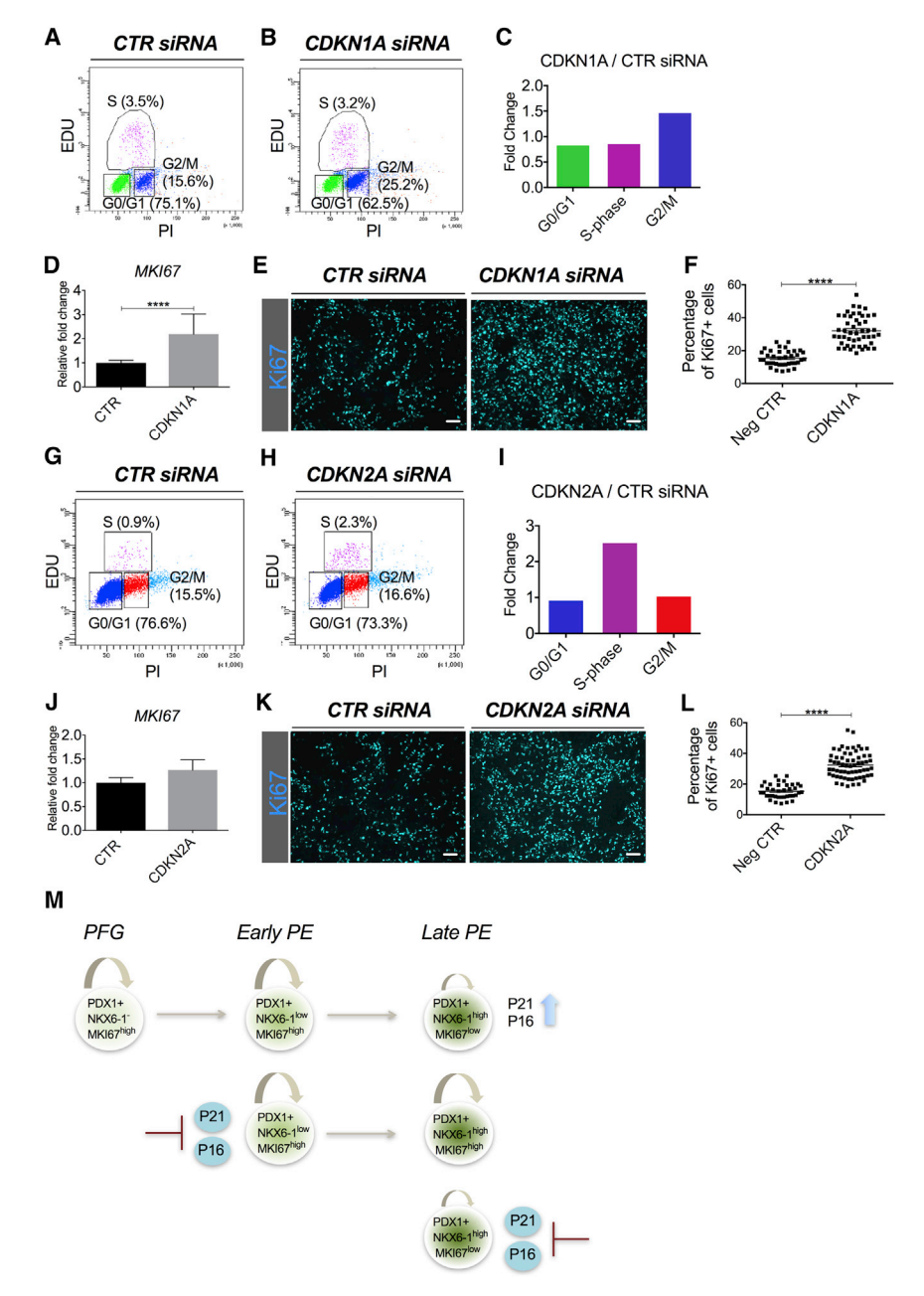


Figure 7. CDKN1A and CDKN2A Knockdown Promotes Proliferation of hESC-**Derived PECs** 

(A and B) Cell-cycle analysis of differentiated hESCs at day 14 corresponding to early PECs. Cells from day 11 were transfected with CDKN1A siRNA, harvested 72 hr later, stained with EdU, and analyzed by flow cytometry (a representative analysis is shown).

- (C) Summary of data depicted in (A) and (B), where the corresponding ratio of CDKN1A/CTR siRNA for each cell-cycle phase is shown.
- (D) qPCR analysis of samples treated with scrambled and CDKN1A siRNA confirmed upregulation of MKI67 expression 24 hr after CDKN1A knockdown. The data are shown as mean expression  $\pm$ SEM. \*\*\*\*p < 0.0001.
- (E) Immunofluorescence analysis confirmed a significant increase of MKI67+ cells 72 hr after knockdown of CDKN1A. Scale bars, 100  $\mu m$ .
- (F) Quantification of MKI67-expressing cells in the cultures showed there was a significant increase in the number of MKI67 $^+$  cells. \*\*\*\*p < 0.0001.
- (G and H) Cells from day 11 were transfected with CDKN2A siRNA, harvested 72 hr later, stained with EdU, and analyzed by flow cytometry (a representative analysis is shown).
- (I) Summary of data depicted in (K) and (L), where the corresponding ratio of CDKN2A/CTR siRNA for each cell-cycle phase is shown.
- (J and K) qPCR analysis showed no statistically significant up-regulation of MKI67 expression in the CDKN2A knocked down samples 24h after transfection, error bars represent mean expression ± SEM (J). However, immunofluorescence analysis showed a significant increase of MKI67+ cells (K) after 72 hr of knockdown of CDKN2A. Scale bars,
- (L) Quantification of MKI67-expressing cells in the cultures confirmed the significant increase in the number of MKI67<sup>+</sup> cells. \*\*\*\*p < 0.0001.
- (M) Schematic displaying PE formation during development. As the PECs mature, CDKN1A (p21) and CDKN2A (p16) expression levels increase and MKI67 expression is downregulated (upper panel). Downregulation of p21 or p16 within early PECs prevents the decrease in proliferation during PE maturation (middle panel), whereas inhibition within late PE is unable to restore proliferation (lower panel).

See also Figures S6 and S7.

transcriptional effect on MKI67 upon reduced CDKN2A levels, compared to CDKN1A. Still, because knocking down the expression of either CDKN1A or CDKN2A promotes proliferation of PECs, they both remain relevant targets for future in vitro expansion of PECs.

We observed that only when the expression of CDKN1A and CDKN2A was decreased in early PECs, proliferation was restored. Previous studies have shown that Neurog3 controls cell-cycle exit in mouse endocrine progenitors at least in part through regulation of CDKN1A expression (Miyatsuka et al.,

<sup>(</sup>C) Co-staining of CPEP (white) and GLU (green) of unsorted cells. Scale bar, 100  $\mu m.\,$ 

<sup>(</sup>D and E) Immunostainings of differentiated GP2<sup>Low</sup> cells (D) and GP2<sup>High</sup> cells (E) with CPEP (white), GLU (green), and NKX6-1 (red). Scale bars, 100 µm.

<sup>(</sup>F) Percentage of CPEP+ cells in unsorted, GP2<sup>Low</sup>, and GP2<sup>High</sup> cells. \*\*\*\* $p \le 0.0001$ .

<sup>(</sup>G) Percentage of GLU $^+$  cells in unsorted, GP2 $^{Low}$ , and GP2 $^{High}$  cells. \*\*\*\*p  $\leq$  0.0001.

<sup>(</sup>H) Static GSIS assay of differentiated GP2High cells showed a 2-fold change in CPEP response. Error bars represent mean expression ± SEM \*\* p ≤ 0.01. See also Figure S5.

2011; Piccand et al., 2014). Time course analysis of differentiated hESCs indicates that NEUROG3 transcription is initiated in the late PECs (data not shown), suggesting that NEUROG3 may be responsible for the sustained expression of at least CDKN1A in the late PECs. However, because knocking down the expression of CDKN1A and CDKN2A in late PECs is not sufficient to reinstate the proliferative capacity of these cells, additional modulators downstream of NEUROG3 must be involved in regulating proliferation and cell-cycle exit in late PECs.

Future clinical trials aiming to test the safety and efficacy of hPSCs-derived beta cells in type 1 diabetes will profit from implementing cost-effective strategies for cell purification. We envision that using isolated GP2+ PECs for derivation of insulin-producing cells for clinical use will significantly improve the safety of the final product. Furthermore, GP2+ PECs can be used to establish an intermediate-stage stem cell bank, permitting the use of more mature yet proliferative cells as a source of functional beta cells. Thus, future studies will need to focus on identifying conditions for in vitro expansion of GP2+ PECs. We foresee a strategy that combines pharmacological targeting of the underlying machinery that regulates proliferation through CDKN1A and/or CDKN2A with growth-promoting signals, such as FGFs and EGF. Once this has been achieved, additional experiments will be required to characterize the maintenance of the PEC phenotype, as well as the capacity to differentiate into functional beta cells over sequential passages.

#### **EXPERIMENTAL PROCEDURES**

#### **Cell Culture and Differentiation**

The PDXeG clone 170-3 was maintained on mouse embryonic fibroblasts (MEFs) in medium containing knockout (KO)-DMEM, 10% knockout serum replacement (KO-SR), 10 ng/mL basic fibroblast growth factor also known as FGF2 (bFGF), 1% non-essential amino acids (NEAAs), 1% Glutamax, and beta-mercaptoethanol (all reagents from Life Technologies). HUES4 and the PDXeG clone 170-3 were adapted and maintained in DEF-CS (Takara), whereas MShef-7 was maintained on laminin-521 (LN521, Biolamina) in Nutristem hESC xeno-free (XF) medium (Biological Industries). Detailed information regarding the differentiation protocols can be found in the Supplemental Experimental Procedures.

#### **RNA Extraction and Real-Time qPCR**

Total RNA was extracted with the GenElute Mammalian total RNA kit (Sigma-Aldrich). Reverse transcription was performed with SuperScript III, according to the manufacturer's instructions, using 2.5  $\mu M$  random hexamer and 2.5  $\mu M$ oligo(dT) (Invitrogen). Real-time PCR measurements were performed using the StepOnePlus system (Applied Biosystems) with SuperMix-UDG w/ROX, 400 nM of each primer, and 0.125× SYBR Green I (all reagents from Life Technologies), with the exception of the qPCR data in Figures 5 and 6, which were generated using the LightCycler 480II (Roche) with PowerSYBR Green PCR Master Mix (Applied Biosystems) and 500 nM of each primer. Primer sequences are available as supplemental data (Table S3) and in our previous publication (Ameri et al., 2010). The data are shown as mean expression  $\pm$ SEM. Relative gene expression was determined using ACTB or GAPDH expression as housekeeping genes. When indicated, the control sample was arbitrarily set to a value of one in the graphs representing the fold increase in comparison to the control sample.

#### **Microarray Analysis of PDXeG Sorted Populations**

Four replicates for each sample were collected by fluorescence-activated cell sorting (FACS). RNA isolation was performed with the GenElute Mammalian total RNA kit (Sigma-Aldrich). cDNA was synthesized and amplified using Ovation RNA amplification system (NuGEN) according to the manufacturer's instructions. The labeled samples were hybridized to the Human Gene 1.0 ST GeneChip array (Affymetrix). The arrays were washed, stained with phycoerythrin-conjugated streptavidin (SAPE) using the Affymetrix Fluidics Station 450, and scanned in the Affymetrix GeneArray 3000 7G scanner to generate fluorescent images, as described in the Affymetrix GeneChip protocol. Cell intensity files (CEL files) were generated in the GeneChip Command Console Software (Affymetrix Genechip Command Console [AGCC]) (Affymetrix). Additional information can be found in the Supplemental Experimental Procedures.

#### **Glucose-Stimulated Insulin Secretion Assay**

Late-stage cultures of differentiated hESCs were washed twice with Krebs-Ringer bicarbonate buffer (KRB) containing 2 mM glucose. Samples were incubated for 2 hr in 2 mM glucose containing KRB to allow equilibration of cells. Fresh KRB containing 2 mM glucose was added, cells were incubated for 30 min, medium was collected, and then cells were washed and incubated for 30 min in KRB containing 25 mM glucose. Medium was collected, and then cells were washed again and incubated with final KRB containing 2 mM glucose and 25 mM KCl. All samples were analyzed for human C-peptide content using a commercially available kit from Mercodia.

#### siRNA Knockdown in Differentiated hESCs

Differentiated hESCs corresponding to day 11 or day 17 were dissociated and transfected with 40 nM CDKN1A, CDKN2A, or scrambled siRNA control (Silencer Select siRNA, Thermo Fisher Scientific) using Lipofectamine RNAiMAX (Thermo Fisher Scientific). 24 hr after transfection, cells were harvested for qPCR; 72 hr later, cells were harvested for immunostainings or western blot analysis and/or treated with EdU for cell-cycle analysis. Immunofluorescence stainings were analyzed with a Leica AF6000 epifluorescence widefield screening microscope.

#### **Cell-Cycle Analysis by Flow Cytometry**

For cell-cycle analysis with flow cytometry, cells were incubated with EdU (5-ethynyl-2'-deoxyuridine) at a concentration of 10 μM for 4 hr before dissociation. Collected samples were live stained with GP2 and fixed with 4% paraformaldehyde (PFA). EdU was revealed by the Click-it EdU Alexa 647 Flow Cytometry Assay kit (Invitrogen). Compatible phosphatidylinositol (PI) staining was added to visualize the cell-cycle profile based on DNA content. Analysis was performed using BD LSR Fortessa (BD Biosciences). 10,000 events were recorded, and doublets were excluded.

### **Data Analysis and Statistics**

Fiji (ImageJ) software was used for all quantifications. The percentage of CPEP+ and GLU+ cells was calculated by measuring the area of CPEP or GLU over the DAPI area. The percentage of MKI67+ cells was calculated by measuring the area of MKI67 over the area of PDX1. The total area was estimated by PDX1 antibody staining and DAPI. The percentage of PECs was quantified by measuring the area of NKX6-1 over the PDX1 area. 20-25 randomly selected fields were chosen for each parameter. All data were statistically analyzed by unpaired or paired Student's t test or by multivariate comparison (one-way ANOVA) with Bonferroni correction using GraphPad Prism 6 software. All values are depicted as mean  $\pm$  SEM and considered significant if p < 0.05.

# **ACCESSION NUMBERS**

The accession number for the microarray data reported in this paper is ArrayExpress: E-MTAB-5088.

#### SUPPLEMENTAL INFORMATION

Supplemental Information includes Supplemental Experimental Procedures, seven figures, and three tables and can be found with this article online at http://dx.doi.org/10.1016/j.celrep.2017.03.032.



#### **AUTHOR CONTRIBUTIONS**

J.A. and H.S. conceived and designed the experiments. J.A. performed the experiments in all figures and supplemental figures and analyzed and assembled the data. R.B. performed the microarray and bioinformatics analysis in Figure 2. C.P. performed the differentiation experiments and qPCR in Figures 4, S3C, and S3D and EdU stainings in Figures 7, S6, and , S7. C.R. and R.S. designed the experiments with the human fetal pancreas. C.R. performed the experiments with human fetal pancreas in Figures 3E-3G. K.A.S. performed the qPCR, immunostainings, and western blot analysis in Figures 6, S6, and , S7 and the qPCR in Figure S1D. J.A., K.A.S., and H.S. wrote the manuscript.

#### **ACKNOWLEDGMENTS**

We thank Dr. Oliver Lieven for valuable comments of the manuscript. We also thank the following for their contributions: Dr. Douglas Melton for supplying hESC lines, University of Sheffield for supplying MShef-7, BCBC core facility for supplying antibodies, Jeanette Løkkegaard and Jette Pia Larsen for excellent assistance with hESC expansion and differentiation experiments, Zhi Ma and Teona Roschupkina from Lund FACS core facility, and Gelo de la Cruz and Paul van Dieken from DanStem FACS core facility. This work has been supported by the Swedish Foundation for Strategic Research, Center for Stem Cell Biology and Cell Therapy, Lund University, Juvenile Diabetes Research Foundation, Novo Nordisk Foundation, Danish Council for Strategic Research. and HumEn project funded by the European Commission's Seventh Framework Programme for Research (agreement 602587). J.A. and H.S. are inventors of an international patent application (WO 2016/170069 A1) based on this work.

Received: October 10, 2016 Revised: February 10, 2017 Accepted: March 9, 2017 Published: April 4, 2017

#### **REFERENCES**

Ameri, J., Ståhlberg, A., Pedersen, J., Johansson, J.K., Johannesson, M.M., Artner, I., and Semb, H. (2010). FGF2 specifies hESC-derived definitive endoderm into foregut/midgut cell lineages in a concentration-dependent manner. Stem Cells 28, 45-56.

Attali, M., Stetsyuk, V., Basmaciogullari, A., Aiello, V., Zanta-Boussif, M.A., Duvillie, B., and Scharfmann, R. (2007). Control of beta-cell differentiation by the pancreatic mesenchyme. Diabetes 56, 1248-1258.

Besson, A., Dowdy, S.F., and Roberts, J.M. (2008). CDK inhibitors: cell cycle regulators and beyond. Dev. Cell 14, 159-169.

Bhushan, A., Itoh, N., Kato, S., Thiery, J.P., Czernichow, P., Bellusci, S., and Scharfmann, R. (2001). Fgf10 is essential for maintaining the proliferative capacity of epithelial progenitor cells during early pancreatic organogenesis. Development 128, 5109-5117.

Bonfanti, P., Nobecourt, E., Oshima, M., Albagli-Curiel, O., Laurysens, V., Stangé, G., Sojoodi, M., Heremans, Y., Heimberg, H., and Scharfmann, R. (2015). Ex vivo expansion and differentiation of human and mouse fetal pancreatic progenitors are modulated by epidermal growth factor. Stem Cells Dev. 24, 1766-1778.

Bruni, A., Gala-Lopez, B., Pepper, A.R., Abualhassan, N.S., and Shapiro, A.J. (2014). Islet cell transplantation for the treatment of type 1 diabetes: recent advances and future challenges. Diabetes Metab. Syndr. Obes. 7, 211-223.

Castaing, M., Duvillié, B., Quemeneur, E., Basmaciogullari, A., and Scharfmann, R. (2005). Ex vivo analysis of acinar and endocrine cell development in the human embryonic pancreas. Dev. Dyn. 234, 339-345.

Cheng, X., Ying, L., Lu, L., Galvão, A.M., Mills, J.A., Lin, H.C., Kotton, D.N., Shen, S.S., Nostro, M.C., Choi, J.K., et al. (2012). Self-renewing endodermal progenitor lines generated from human pluripotent stem cells. Cell Stem Cell 10, 371-384.

Donovan, J., and Slingerland, J. (2000). Transforming growth factor-beta and breast cancer: cell cycle arrest by transforming growth factor-beta and its disruption in cancer. Breast Cancer Res. 2, 116-124.

Elghazi, L., Cras-Méneur, C., Czernichow, P., and Scharfmann, R. (2002). Role for FGFR2IIIb-mediated signals in controlling pancreatic endocrine progenitor cell proliferation. Proc. Natl. Acad. Sci. USA 99, 3884-3889.

Gu, G., Dubauskaite, J., and Melton, D.A. (2002). Direct evidence for the pancreatic lineage: NGN3+ cells are islet progenitors and are distinct from duct progenitors. Development 129, 2447-2457.

Guo, T., Landsman, L., Li, N., and Hebrok, M. (2013). Factors expressed by murine embryonic pancreatic mesenchyme enhance generation of insulin-producing cells from hESCs. Diabetes 62, 1581-1592.

Herrera, P.L. (2002). Defining the cell lineages of the islets of Langerhans using transgenic mice. Int. J. Dev. Biol. 46, 97-103.

Hoops, T.C., and Rindler, M.J. (1991). Isolation of the cDNA encoding glycoprotein-2 (GP-2), the major zymogen granule membrane protein. Homology to uromodulin/Tamm-Horsfall protein. J. Biol. Chem. 266, 4257-4263.

Jennings, R.E., Berry, A.A., Kirkwood-Wilson, R., Roberts, N.A., Hearn, T., Salisbury, R.J., Blaylock, J., Piper Hanley, K., and Hanley, N.A. (2013). Development of the human pancreas from foregut to endocrine commitment. Diabetes 62 3514-3522

Kawaguchi, Y., Cooper, B., Gannon, M., Ray, M., MacDonald, R.J., and Wright, C.V. (2002). The role of the transcriptional regulator Ptf1a in converting intestinal to pancreatic progenitors. Nat. Genet. 32, 128-134.

Kelly, O.G., Chan, M.Y., Martinson, L.A., Kadoya, K., Ostertag, T.M., Ross, K.G., Richardson, M., Carpenter, M.K., D'Amour, K.A., Kroon, E., et al. (2011). Cell-surface markers for the isolation of pancreatic cell types derived from human embryonic stem cells. Nat. Biotechnol. 29, 750-756.

Kippin, T.E., Martens, D.J., and van der Kooy, D. (2005). p21 loss compromises the relative quiescence of forebrain stem cell proliferation leading to exhaustion of their proliferation capacity. Genes Dev. 19, 756-767.

Koike, H., Ueno, Y., Naito, T., Shiina, T., Nakata, S., Ouchi, R., Obana, Y., Sekine, K., Zheng, Y.W., Takebe, T., et al. (2014), Ring1B promotes hepatic stem/ progenitor cell expansion through simultaneous suppression of Cdkn1a and Cdkn2a in mice. Hepatology 60, 323-333.

Kopp, J.L., Dubois, C.L., Schaffer, A.E., Hao, E., Shih, H.P., Seymour, P.A., Ma, J., and Sander, M. (2011). Sox9+ ductal cells are multipotent progenitors throughout development but do not produce new endocrine cells in the normal or injured adult pancreas. Development 138, 653-665.

Miyatsuka, T., Kosaka, Y., Kim, H., and German, M.S. (2011). Neurogenin3 inhibits proliferation in endocrine progenitors by inducing Cdkn1a. Proc. Natl. Acad. Sci. USA 108, 185-190.

Nair, G., and Hebrok, M. (2015). Islet formation in mice and men: lessons for the generation of functional insulin-producing β-cells from human pluripotent stem cells. Curr. Opin. Genet. Dev. 32, 171-180.

Orford, K.W., and Scadden, D.T. (2008). Deconstructing stem cell selfrenewal: genetic insights into cell-cycle regulation. Nat. Rev. Genet. 9,

Paqliuca, F.W., Millman, J.R., Gürtler, M., Segel, M., Van Dervort, A., Ryu, J.H., Peterson, Q.P., Greiner, D., and Melton, D.A. (2014). Generation of functional human pancreatic β cells in vitro. Cell 159, 428-439.

Piccand, J., Meunier, A., Merle, C., Jia, Z., Barnier, J.V., and Gradwohl, G. (2014). Pak3 promotes cell cycle exit and differentiation of  $\beta$ -cells in the embryonic pancreas and is necessary to maintain glucose homeostasis in adult mice. Diabetes 63, 203-215.

Rezania, A., Bruin, J.E., Xu, J., Narayan, K., Fox, J.K., O'Neil, J.J., and Kieffer, T.J. (2013). Enrichment of human embryonic stem cell-derived NKX6.1-expressing pancreatic progenitor cells accelerates the maturation of insulinsecreting cells in vivo. Stem Cells 31, 2432-2442.

Rezania, A., Bruin, J.E., Arora, P., Rubin, A., Batushansky, I., Asadi, A., O'Dwyer, S., Quiskamp, N., Mojibian, M., Albrecht, T., et al. (2014). Reversal of diabetes with insulin-producing cells derived in vitro from human pluripotent stem cells. Nat. Biotechnol. 32, 1121-1133.



Russ, H.A., Parent, A.V., Ringler, J.J., Hennings, T.G., Nair, G.G., Shveygert, M., Guo, T., Puri, S., Haataja, L., Cirulli, V., et al. (2015). Controlled induction of human pancreatic progenitors produces functional beta-like cells in vitro. EMBO J. 34, 1759-1772.

Schaffer, A.E., Freude, K.K., Nelson, S.B., and Sander, M. (2010). Nkx6 transcription factors and Ptf1a function as antagonistic lineage determinants in multipotent pancreatic progenitors. Dev. Cell 18, 1022-1029.

Schulz, T.C., Young, H.Y., Agulnick, A.D., Babin, M.J., Baetge, E.E., Bang, A.G., Bhoumik, A., Cepa, I., Cesario, R.M., Haakmeester, C., et al. (2012). A scalable system for production of functional pancreatic progenitors from human embryonic stem cells. PLoS ONE 7, e37004.

Seymour, P.A., Freude, K.K., Tran, M.N., Mayes, E.E., Jensen, J., Kist, R., Scherer, G., and Sander, M. (2007). SOX9 is required for maintenance of the pancreatic progenitor cell pool. Proc. Natl. Acad. Sci. USA 104, 1865-1870.

Sneddon, J.B., Borowiak, M., and Melton, D.A. (2012). Self-renewal of embryonic-stem-cell-derived progenitors by organ-matched mesenchyme. Nature

Stanger, B.Z., Tanaka, A.J., and Melton, D.A. (2007). Organ size is limited by the number of embryonic progenitor cells in the pancreas but not the liver. Nature 445, 886-891.

Xie, R., Everett, L.J., Lim, H.W., Patel, N.A., Schug, J., Kroon, E., Kelly, O.G., Wang, A., D'Amour, K.A., Robins, A.J., et al. (2013). Dynamic chromatin remodeling mediated by polycomb proteins orchestrates pancreatic differentiation of human embryonic stem cells. Cell Stem Cell 12, 224-237.

Ye, F., Duvillié, B., and Scharfmann, R. (2005). Fibroblast growth factors 7 and 10 are expressed in the human embryonic pancreatic mesenchyme and promote the proliferation of embryonic pancreatic epithelial cells. Diabetologia 48. 277-281.

Yoon, M.K., Mitrea, D.M., Ou, L., and Kriwacki, R.W. (2012). Cell cycle regulation by the intrinsically disordered proteins p21 and p27. Biochem. Soc. Trans. 40, 981-988.

Yu, S., Michie, S.A., and Lowe, A.W. (2004). Absence of the major zymogen granule membrane protein, GP2, does not affect pancreatic morphology or secretion, J. Biol. Chem. 279, 50274-50279.

Zhang, D., Jiang, W., Liu, M., Sui, X., Yin, X., Chen, S., Shi, Y., and Deng, H. (2009). Highly efficient differentiation of human ES cells and iPS cells into mature pancreatic insulin-producing cells. Cell Res. 19, 429-438.

Zhu, S., Russ, H.A., Wang, X., Zhang, M., Ma, T., Xu, T., Tang, S., Hebrok, M., and Ding, S. (2016). Human pancreatic beta-like cells converted from fibroblasts. Nat. Commun. 7, 10080.